

# Characterizing an entangled-photon source with classical detectors and measurements

LEE A. ROZEMA,<sup>1,2,\*</sup> CHAO WANG,<sup>1</sup> DYLAN H. MAHLER,<sup>1</sup> ALEX HAYAT,<sup>1,3,4</sup> AEPHRAIM M. STEINBERG,<sup>1,3</sup> JOHN E. SIPE,<sup>1</sup> AND MARCO LISCIDINI<sup>5</sup>

<sup>1</sup>Centre for Quantum Information & Quantum Control and Institute for Optical Sciences, Department of Physics, 60 St. George St., University of Toronto, Toronto, Ontario M5S 1A7, Canada

<sup>2</sup>University of Vienna, Faculty of Physics, Boltzmannngasse 5, 1090 Vienna, Austria

<sup>3</sup>Canadian Institute for Advanced Research, Toronto, Ontario M5G 1Z8, Canada

<sup>4</sup>Department of Electrical Engineering, Technion, Haifa 32000, Israel

<sup>5</sup>Dipartimento di Fisica, Università degli Studi di Pavia, via Bassi 6, I-27100 Pavia, Italy

\*Corresponding author: lee.rozema@univie.ac.at

Received 21 November 2014; revised 19 March 2015; accepted 24 March 2015 (Doc. ID 228363); published 27 April 2015

**Entangled-photon pairs are essential for many applications in quantum computation and communication, and quantum state tomography (QST) is the universal tool to characterize such entangled-photon sources. In QST, very low-power signals must be measured with single-photon detectors and coincidence logic. Here, we experimentally implement a new protocol, “stimulated-emission tomography” (SET), allowing us to obtain the information provided by QST when the photon pairs are generated by parametric fluorescence. This approach exploits a stimulated process that results in a signal several orders of magnitude larger than in QST. In particular, we characterize the polarization state of photons that would be generated in spontaneous parametric downconversion using SET. We find that SET accurately predicts the purity and concurrence of the spontaneously generated photons in agreement with the results of QST. We expect that SET will be extremely useful to characterize entanglement sources based on parametric fluorescence, providing a fast and efficient technique to potentially replace or supplement QST. © 2015 Optical Society of America**

**OCIS codes:** (270.5585) Quantum information and processing; (190.4410) Nonlinear optics, parametric processes.

<http://dx.doi.org/10.1364/OPTICA.2.000430>

Quantum information is an important emerging technology [1], and entanglement is its essential ingredient. It plays a vital role in tasks such as quantum computation [2,3], quantum metrology [4,5], and quantum key distribution [6], and so the development of high-quality entanglement sources is of central importance for quantum information technology.

For any source of entangled states to be useful, it must be characterized. The standard method for doing this is quantum state tomography (QST) [7]. In principle, QST provides a complete description of the quantum state, from which one can evaluate

the suitability of a source for any proposed application. But it is well known that QST is a resource-intensive task. The quality of the tomographic estimate depends on the amount of data that one is able to acquire [8–10] and analyze [11], with more data typically resulting in a higher-quality estimate.

In this Letter, we investigate a particular physical system—entangled-photon pairs generated via spontaneous parametric downconversion (SPDC) in a pair of BBO crystals—and show how the corresponding stimulated process, namely difference frequency generation (DFG), can be used to reconstruct the polarization density matrix of the two-photon state that arises in the spontaneous process. The signal generated by DFG can be several orders of magnitude more intense than that observed in SPDC, making it possible to estimate the quantum states produced by such sources very rapidly and efficiently [12]. This is particularly important en route to the development of “on-chip” sources of entangled states [13–15]; as in the case of integrated electronic circuits, such sources are typically produced in large numbers, and fast and efficient characterization procedures are required. The approach of “stimulated-emission tomography” (SET) that we demonstrate here would allow for the full quantum characterization of sources with low photon-pair generation rates, for which characterization by QST might not be feasible. While an experiment exploiting the relation between stimulated and spontaneous emission to measure spectral correlations between the spontaneously generated photons has been performed recently [16,17], the full tomography of photon pairs using SET has yet to be demonstrated. That is what we undertake here.

As a test case for SET, we use our polarization-entangled-photon source (an SPDC “sandwich source” [18]), which is illustrated in Fig. 1(a); here a pair of nonlinear birefringent crystals is mounted with their optic axes orthogonal. In an idealized picture, when a diagonally polarized pump pulse is incident the first crystal could produce pairs of horizontally polarized photons in the signal and idler modes (taking  $|V\rangle_p \rightarrow |HH\rangle_{s,i}$ ), or the second crystal could produce vertically polarized photon pairs (taking  $|H\rangle_p \rightarrow |VV\rangle_{s,i}$ ). Thus, if the source—i.e., the pump

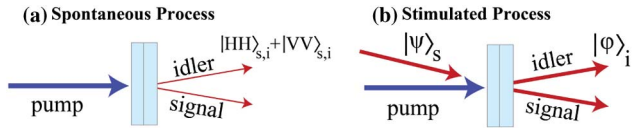


**Fig. 1.** (a) Simple cartoon of a SPDC “sandwich” source that produces entangled-photon pairs. (b) Stimulated version of the SPDC sandwich source; now a seed beam is sent into the signal mode to stimulate light into the idler mode.

pulse, the nonlinear crystals, and the collection optics—is appropriately configured [19,20], SPDC results in the generation of a polarization-entangled state  $(|HH\rangle_{s,i} + |VV\rangle_{s,i})/\sqrt{2}$ .

To characterize this state using QST, the polarization of each photon is measured in several different bases. Experimentally, this is typically done by sending each photon to a set of waveplates and a polarizer [Fig. 2(b)], and estimating the probability that both photons are transmitted. For example, if both polarizers are aligned in the horizontal direction, we can estimate  $\mathcal{P}_{H,H}$ . For two-photons, 16 such probabilities are sufficient to constrain the two-photon polarization state. Thus, these measurements can be used to estimate the two-photon polarization density matrix [7]; see Supplement 1 for more details.

In SET, a strong seed beam is constructed to mimic the signal photons of the pair that could be generated by spontaneous emission [Fig. 1(b)], including all possible polarizations. It is important that during SET only this seed beam is changed, and the source is not manipulated at all. Consequently, in the presence of the seed beam, an idler beam is generated by DFG. Two of us predicted earlier that the biphoton wavefunction characterizing the pairs that would be emitted by SPDC acts as the response function relating the idler beam to the seed beam in DFG (see Ref. [12] for a full theoretical treatment). Thus, by changing the polarization of a properly configured seed beam  $|\psi\rangle_s$ , and performing measurements on the polarization of the stimulated idler  $|\phi\rangle_i$ , conclusions can be drawn about the two-photon state that would be generated in the absence of the seed. For example, using a horizontally polarized seed beam and measuring the stimulated

beam in the horizontal basis, one can compute the probability of detecting a horizontally polarized signal photon and a horizontally polarized idler photon in a spontaneous experiment  $\mathcal{P}_{H,H}$ . In an ideal situation, this probability is simply  $\mathcal{P}_{H,H} = I_H^{\text{stim}}/I_H^{\text{seed}}$ , where  $I_H^{\text{stim}}$  is the intensity of the horizontally polarized stimulated light and  $I_H^{\text{seed}}$  is the intensity of the seed light. In experiment, however, additional steps must be taken to normalize the data (see Supplement 1). This procedure can be repeated for other polarization combinations, yielding the same information as QST. Thus, SET obtains sufficient information to reconstruct the full two-photon polarization state generated in a spontaneous experiment. To be clear, both SET and QST only predict this state, not other properties of the source.

The source and our implementation of QST and SET are shown in Fig. 2. Our sandwich crystals are a pair of 1-mm-thick BBO crystals. To generate entangled photons, a “temporal compensation” crystal is placed before the sandwich crystals to pre-delay one component of the pump polarization so that, by the time the photon pairs emerge from the sandwich crystals, the  $|H, H\rangle_{s,i}$  pairs are temporally indistinguishable from the  $|V, V\rangle_{s,i}$  pairs. Our source is pumped with  $\approx 200$ -fs-long pulses that are centred at 400 nm, with an average power of 500 mW. This pump light is generated by frequency-doubling 1.5 W (average power) of 800 nm light from a femtosecond Ti:sapphire laser with a 76 MHz repetition rate, using a 2-mm-long BBO crystal. The 400 nm pump pulse is focused into the crystal with a 15 cm lens, resulting in a beam waist of  $\approx 50 \mu\text{m}$  in the crystal.

The collected signal and idler modes are defined by two single-mode fibers (with a numerical aperture of 0.12), a 10 cm focal-length lens to collimate the emission, and two 4 mm aspherical lenses to focus the signal and idler beams into the fiber. Light is collected from a spot size that is about the same size as the focused pump, as prescribed in Ref. [21]. Finally, each mode is filtered with a 10 nm spectral filter centred at 800 nm. This produces  $\approx 15,000$  polarization-entangled photon pairs per second coupled in the signal and idler modes, with a coupling efficiency (pairs/singles) of  $\approx 15\%$ . These photons are directed to a standard QST apparatus [see Fig. 2(b)], where the photon pairs are detected with single-photon detectors, and coincidence counts are registered with a homebuilt FPGA-based coincidence circuit. When the source is nominally configured to generate the maximally entangled state  $(|HH\rangle_{s,i} + |VV\rangle_{s,i})/\sqrt{2}$ , QST yields the polarization density matrix shown in Fig. 3(a), which has a fidelity of  $\approx 0.951$  with the maximally entangled state.

To perform SET, a seed field is constructed by diverting approximately 150 mW of the original 800 nm pulsed Ti:sapphire light; in this configuration, the 400 nm average pump power is also 150 mW. Note that this is not a strict application of SET as proposed earlier [12], since it makes use of a pulsed seed and not a CW seed. This can introduce errors in the determination of the polarization density matrix when the biphoton wavefunction depends strongly on the photon energy within the seed pulse bandwidth (see Ref. [12] for more details). To compensate for this, we used a 3 nm spectral filter to lengthen the seed pulse. Finally, since the pump and the seed pulse have different frequencies, they experience different spatial walk-offs. To minimize this effect the seed beam waist is made much larger than the pump beam waist (approximately 1000  $\mu\text{m}$ ), so that good spatial overlap is maintained as both beams traverse the nonlinear crystals. Note that if the “seed lens” [Fig. 2(a)] is removed, then the seed pulse would

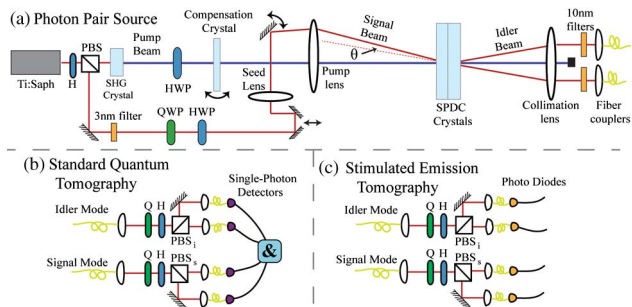


**Fig. 2.** (a) Our entangled-photon source and the generation of our seed beam for stimulated-emission tomography (SET). The signal and idler modes are coupled into single-mode fibers, and sent to a tomography apparatus. (b) The standard quantum tomography apparatus consists of a pair of polarization measurements on each mode (implemented using waveplates and polarizing beamsplitter cubes). The output modes of each cube are coupled to single-photon detectors, and coincidences between detectors are monitored. (c) The SET apparatus is almost identical to the quantum tomography apparatus, but photodiodes replace the single-photon detectors, and there are no coincidence measurements.

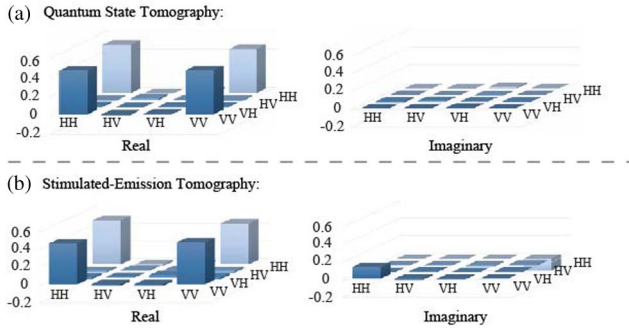


**Fig. 3.** Two-photon density matrices reconstructed by (a) standard QST and (b) SET. The SET reconstruction is based on the single-photon density matrices shown in Table 1 of Supplement 1. The density matrices reconstructed using the two methods have a fidelity of 0.963 with each other.

have a waist of 50  $\mu\text{m}$  in the crystal; in this configuration the different spatial walk-offs become relevant. As we discuss in Section 3 of Supplement 1, this can lead to polarization-dependent losses, which can introduce errors in the SET reconstruction. When the 1000  $\mu\text{m}$  seed beam is temporally and spatially overlapped with the pump pulse in the SPDC crystals, we observe a stimulated idler output power of approximately 100  $\mu\text{W}$  coupled into the single-mode fiber. The polarization measurements for SET are then performed in the same apparatus used for QST, but with the single-photon detectors replaced by photodiodes [Fig. 2(c)].

We prepare the seed signal pulse in six different polarization states, and, for each, we measure the intensity of the stimulated idler in the same six polarization states (see Table 1 of Supplement 1). These data are fed into our least-squares fitting algorithm (presented in Supplement 1) to reconstruct the quantum state. When the source is nominally configured to generate the maximally entangled state  $(|HH\rangle_{s,i} + |VV\rangle_{s,i})/\sqrt{2}$ , SET yields the density matrix shown in Fig. 3(b), which has a fidelity of  $\approx 0.939$  with the maximally entangled state.

The results of QST and SET are close but significantly different; the quantum fidelity of one with respect to the other is 0.963 [22]. The difference arises because the phases between  $|HH\rangle_{s,i}$  and  $|VV\rangle_{s,i}$  extracted by SET and QST disagree by 0.289 rad; this is manifest in the larger imaginary components in the SET prediction. Were the phases artificially set to be identical, the fidelity between the two estimates would increase to 0.982.

We will return to the disagreement between QST and SET below, but first note that measures of entanglement (such as concurrence) are not sensitive to the phase between  $|HH\rangle_{s,i}$  and  $|VV\rangle_{s,i}$ . Hence, we should expect that QST and SET would predict essentially the same amount of entanglement.

To confirm this, in one set of experiments we prepare states of the form  $\alpha|HH\rangle_{s,i} + \beta|VV\rangle_{s,i}$  and vary  $|\alpha|^2$  from  $1/\sqrt{2}$  to 0 (by rotating the pump polarization with a half waveplate). This gradually decreases the concurrence of the source (while keeping the state approximately pure). We perform both SET and QST on states in this range; the concurrences predicted by both techniques are plotted versus  $|\alpha|^2$  in Fig. 4(a). Since the concurrence is independent of the phase between  $|HH\rangle_{s,i}$  and  $|VV\rangle_{s,i}$ , the QST and SET results agree extremely well.

The most common problem plaguing polarization-entanglement sources is a reduced coherence between  $|HH\rangle_{s,i}$

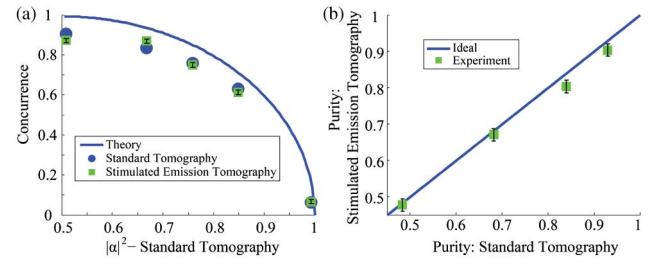


**Fig. 4.** (a) Plot of the concurrence versus  $|\alpha|^2$ ;  $|\alpha|^2$  was extracted from QST. These data were taken for entangled states of the nominal form  $\alpha|HH\rangle + \beta|VV\rangle$ . The green squares were extracted from SET, the blue circles are from QST, and the blue curve is a simple theory calculation assuming perfectly pure states. (b) Plot of the purity extracted from SET versus the purity extracted from standard QST. For these data  $|\alpha|^2 \approx 0.5$ , and the compensation crystal in the source was systematically misaligned to reduce the purity.

and  $|VV\rangle_{s,i}$ , which results in a loss of entanglement [20]. Therefore, we performed a second set of experiments, showing that SET can characterize this loss. In sandwich sources pumped with an ultrafast laser, such as ours, the entanglement is often reduced by imperfect temporal compensation; the  $|HH\rangle_{s,i}$  and  $|VV\rangle_{s,i}$  photons are emitted in distinguishable temporal modes, so that ignoring these temporal modes effectively decoheres the state. To see how QST and SET capture this loss of polarization entanglement, we initially set (using QST) our source to produce the nominal state  $(|HH\rangle_{s,i} + |VV\rangle_{s,i})/\sqrt{2}$  with high purity, and then began to misalign the compensation crystal to reduce the purity of the states. For the highest purity data point the compensation crystal was nominally aligned; the two subsequent data points were acquired with the crystal rotated about the vertical axis to  $10^\circ$  and then to  $20^\circ$ , while for the final data point the compensation crystal was removed altogether. Both QST and SET were performed on these states, and the purities yielded by the two techniques are in good agreement, as shown in Fig. 4(b). Again, this agreement is independent of the actual phase between  $|HH\rangle_{s,i}$  and  $|VV\rangle_{s,i}$ .

We now return to the disagreement in the phase between QST and SET. A deeper investigation allowed us to establish that the phase between  $|HH\rangle_{s,i}$  and  $|VV\rangle_{s,i}$  extracted by SET is a function of the incidence angle of the seed ( $\theta$  in Fig. 2) as illustrated in Fig. 5. In particular, it varies by  $\approx 0.312$  rad per mrad deviation of the seed (extracted from the fit). This is simply because the spontaneously generated photons can be emitted at different angles, and the crystals are birefringent. The magnitude of our measured

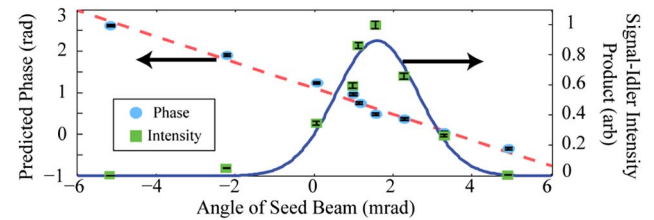


**Fig. 5.** Effect of the seed angle. The circles represent the phase of the entangled state predicted by SET plotted versus the seed incidence angle. The dashed line is a fit to these data, indicating a phase change of 0.312 rad per mrad. The squares represent the product of the intensity of the signal and idler light coupled into the fiber. The solid curve is a Gaussian fit to these data.

angle-dependent phase agrees well with the theory of Ref. [19], which predicts 0.461 rad per mrad.

In our QST experiment, pairs are collected over a transverse momentum range  $\Delta k_f = \lambda/(\pi\omega_f) \approx 5$  mrad, which can be estimated by observing that the single-mode fibers collect from a spot size of  $\omega_f \approx 50$   $\mu\text{m}$  in the crystal; the angular phase-matching bandwidth of our SPDC crystals is  $\approx 3.5$  mrad [23]. Thus, the polarization matrix determined by QST is the result of averaging over the emission angles, and the identification of a state [as in Fig. 3(a)] such as  $(|HH\rangle_{s,i} + |VV\rangle_{s,i})/\sqrt{2}$  indeed is truly only nominal; in fact, there is entanglement between polarization degrees of freedom and emission angle. This is a well-known result in bulk SPDC, where one often collects pairs over a broad range to increase the detection rate [19,20].

In contrast, in SET our seed pulse has a waist of  $\omega_s \approx 1000$   $\mu\text{m}$ , with a range in transverse momenta of only  $\Delta k_s \approx 0.3$  mrad. Thus, one can selectively explore the density matrix of pairs generated at specific angles, so that SET can easily capture the effect of the phase dependence on the emission angle. Hence SET will allow us to investigate the biphoton wavefunction that would be generated by SPDC in even more detail than the usual, emission-angle averaged QST. In fact, the disagreement with QST [as in comparing Figs. 3(a) and 3(b)] can be understood as the ability of SET to look “deeper” into the biphoton wavefunction than standard QST, and actually study the entanglement between polarization and emission angle. It should be possible to obtain the SET results [Fig. 3(b)] with QST, by restricting the collection of pairs over the SET angular ranges. While this has been studied [19], it leads to a considerably decreased coincidence rate, making QST in this situation very time consuming and often impractical. We will return to these kinds of characterizations in the future; in fact, it has already been reported [16,17] that the extraction of frequency correlations can be done with a much higher resolution in a stimulated experiment.

In conclusion, we have experimentally demonstrated that sources of entangled photons generated by SPDC can be characterized using a technique based on stimulated emission, SET. This allowed us to perform a sort of virtual tomography of the quantum correlated pairs that would be generated were the stimulating seed beam absent. Especially in low-count-rate sources, SET should allow for a faster, less demanding, and more accurate characterization of sources of entangled photon pairs than standard QST. A high fidelity between the quantum state deduced from SET and that deduced from QST was found. Differences between the results of SET and QST can be understood as arising from the emission-angle averaging that results in usual QST. Using SET it should be possible to reveal the

underlying structure of the polarization-angle correlations, revealing an entanglement between polarization and emission angle to which a usual application of QST is blind.

Natural Sciences and Engineering Research Council of Canada (NSERC); The Canadian Institute for Advanced Research (CIFAR).

See Supplement 1 for supporting content.

## REFERENCES

1. M. A. Nielsen and I. L. Chuang, *Quantum Computation and Quantum Information* (Cambridge University, 2000).
2. R. Raussendorf, D. E. Browne, and H. J. Briegel, *Phys. Rev. A* **68**, 022312 (2003).
3. P. Walther, K. J. Resch, T. Rudolph, E. Schenck, H. Weinfurter, V. Vedral, M. Aspelmeyer, and A. Zeilinger, *Nature* **434**, 169 (2005).
4. A. N. Boto, P. Kok, D. S. Abrams, S. L. Braunstein, C. P. Williams, and J. P. Dowling, *Phys. Rev. Lett.* **85**, 2733 (2000).
5. M. W. Mitchell, J. S. Lundeen, and A. M. Steinberg, *Nature* **429**, 161 (2004).
6. A. K. Ekert, *Phys. Rev. Lett.* **67**, 661 (1991).
7. D. F. V. James, P. G. Kwiat, W. J. Munro, and A. G. White, *Phys. Rev. A* **64**, 052312 (2001).
8. R. D. Gill and S. Massar, *Phys. Rev. A* **61**, 042312 (2000).
9. R. Okamoto, M. Iefuji, S. Oyama, K. Yamagata, H. Imai, A. Fujiwara, and S. Takeuchi, *Phys. Rev. Lett.* **109**, 130404 (2012).
10. D. H. Mahler, L. A. Rozema, A. Darabi, C. Ferrie, R. Blume-Kohout, and A. M. Steinberg, *Phys. Rev. Lett.* **111**, 183601 (2013).
11. D. Gross, Y.-K. Liu, S. T. Flammia, S. Becker, and J. Eisert, *Phys. Rev. Lett.* **105**, 150401 (2010).
12. M. Liscidini and J. E. Sipe, *Phys. Rev. Lett.* **111**, 193602 (2013).
13. R. Horn, P. Abolghasem, B. J. Bijlani, D. Kang, A. S. Helmy, and G. Weihs, *Phys. Rev. Lett.* **108**, 153605 (2012).
14. A. Orioux, A. Eckstein, A. Lemaitre, P. Filloux, I. Favero, G. Leo, T. Coudreau, A. Keller, P. Milman, and S. Ducci, *Phys. Rev. Lett.* **110**, 160502 (2013).
15. R. T. Horn, P. Kolenderski, D. Kang, P. Abolghasem, C. Scarcella, A. Della Frera, A. Tosi, L. G. Helt, S. V. Zhukovsky, J. E. Sipe, G. Weihs, A. S. Helmy, and T. Jennewein, *Sci. Rep.* **3**, 2314 (2013).
16. A. Eckstein, G. Boucher, A. Lemaitre, P. Filloux, I. Favero, G. Leo, J. E. Sipe, M. Liscidini, and S. Ducci, *Laser Photon. Rev.* **8**, L76 (2014).
17. B. Fang, O. Cohen, M. Liscidini, J. E. Sipe, and V. O. Lorenz, *Optica* **1**, 281 (2014).
18. P. G. Kwiat, K. Mattle, H. Weinfurter, A. Zeilinger, A. V. Sergienko, and Y. Shih, *Phys. Rev. Lett.* **75**, 4337 (1995).
19. J. Altepeter, E. Jeffrey, and P. Kwiat, *Opt. Express* **13**, 8951 (2005).
20. R. Rangarajan, M. Goggin, and P. Kwiat, *Opt. Express* **17**, 18920 (2009).
21. A. Ling, A. Lamas-Linares, and C. Kurtsiefer, *Phys. Rev. A* **77**, 043834 (2008).
22. R. Jozsa, *J. Mod. Opt.* **41**, 2315 (1994).
23. SNLO nonlinear optics code available from A. V. Smith, AS-Photonics, Albuquerque, New Mexico, USA.